Patrick Charlot: Modeling Radio Source Structure for Improved VLBI Data Analysis, IVS 2002 General Meeting Proceedings, p.233–242
http://ivscc.gsfc.nasa.gov/publications/gm2002/charlot

Modeling Radio Source Structure for Improved VLBI Data Analysis

Patrick Charlot

Observatoire de Bordeaux – CNRS/UMR 5804
e-mail: charlot@observ.u-bordeaux.fr

Abstract

At the milliarcsecond scale, most of the extragalactic radio sources exhibit spatially extended intrinsic structures which are variable in both time and frequency. Such radio structures may introduce sizeable effects in the VLBI measurements which must be corrected for improved VLBI data analysis. Modeling these effects requires identification of a truly kinematically stable morphological feature for each source and calculation of structure corrections for the VLBI delays based on images of the source brightness distribution. This paper presents the model for calculating source structure corrections, discusses the magnitude of these corrections, and reviews the results obtained so far, with emphasis on a detailed study of the structural effects caused by the source 2200+420 in the framework of the massive analysis reported by Sovers et al. in these proceedings.

1. Introduction

Current limitation of VLBI data analysis is caused predominantly by troposphere and instrumental errors, but also at some level by the extended brightness distribution of the observed radio sources, which are only imperfect fiducial points in the sky at the milliarcsecond (mas) scale [1, 2, 3]. Such radio structures give rise to structural VLBI delays which vary with the length and orientation of the VLBI baselines relative to the source brightness distribution, causing extra "noise" for the more extended sources. Temporal evolution of these structures may also result in apparent source position variations when observations are made at several epochs [4].

While structural effects may be considered as an intrinsic limitation of the extragalactic radio reference frame, it is worthwhile to try modeling them to further improve the accuracy of the celestial frame and reduce VLBI analysis errors. This requires that a true kinematically-stable feature be identified within each extended source, to serve as the source reference direction. The theoretical basis for such modeling is presented in Section 2, followed by comments about the selection of the source reference direction (Section 3). The magnitude of source structure effects is discussed in Section 4, with emphasis on the definition of the structure index, an indicator of the source quality. Finally, in Section 5, we review the results obtained so far when modeling structural delays in actual data, including a detailed report about recent work on the source 2200+420.

2. Theoretical Modeling

The complex visibility V of a spatially-extended source measured by an interferometer with baseline $\boldsymbol{b}$ is given by

$$V(\boldsymbol{b},\omega,t) = \int_{\Omega_s} I(\boldsymbol{s},\omega,t) \exp\left(-\frac{i\omega}{c}\,\boldsymbol{b}\cdot\boldsymbol{s}\right) d\Omega\,, \qquad (1)$$

where $I(\boldsymbol{s},\omega,t)$ is the source brightness distribution which depends on the direction $\boldsymbol{s}$ on the sky, the frequency $\omega = 2\pi c/\lambda$, and time t, while the integration is over the extended source of solid angle Ω_s. If we adopt a reference direction $\boldsymbol{s_0}$ within the source, $\boldsymbol{s}$ can be written as $\boldsymbol{s} = \boldsymbol{s_0} + \boldsymbol{\sigma}$, where $\boldsymbol{\sigma}$ is in the plane of the sky. The visibility function then can be written as

$$V(\boldsymbol{b},\omega,t) = \exp\left(-\frac{i\omega}{c}\,\boldsymbol{b}\cdot\boldsymbol{s_0}\right)\int_{\Omega_s} I(\boldsymbol{s_0}+\boldsymbol{\sigma},\omega,t)\exp\left(-\frac{i\omega}{c}\,\boldsymbol{b}\cdot\boldsymbol{\sigma}\right)d\Omega\,, \tag{2}$$

which also can be written as

$$\begin{aligned} V &= A\exp[i(\phi_g+\phi_s)]\,, \\ &= A\exp(i\phi_t)\,, \end{aligned} \tag{3}$$

where the total phase ϕ_t is the sum of the geometric phase for the reference direction $\boldsymbol{s_0}$,

$$\phi_g = -\frac{\omega}{c}\,\boldsymbol{b}\cdot\boldsymbol{s_0}\,, \tag{4}$$

and the additional structure phase introduced by the source brightness distribution,

$$\phi_s = \arg\left[\int_{\Omega_s} I(\boldsymbol{s_0}+\boldsymbol{\sigma},\omega,t)\exp\left(-\frac{i\omega}{c}\,\boldsymbol{b}\cdot\boldsymbol{\sigma}\right)d\Omega\right]\,. \tag{5}$$

The amplitude A observed by the interferometer is given by

$$A = \left|\int_{\Omega_s} I(\boldsymbol{s_0}+\boldsymbol{\sigma},\omega,t)\exp\left(-\frac{i\omega}{c}\,\boldsymbol{b}\cdot\boldsymbol{\sigma}\right)d\Omega\right|\,. \tag{6}$$

The VLBI delay observable used in astrometry is defined by the partial derivative of the total phase with respect to frequency. For an extended source, the delay can be written as

$$\begin{aligned} \tau &= \frac{\partial\phi_t}{\partial\omega} = \frac{\partial\phi_g}{\partial\omega} + \frac{\partial\phi_s}{\partial\omega}\,, \\ &= -\frac{1}{c}\,\boldsymbol{b}\cdot\boldsymbol{s_0} + \tau_s\,, \end{aligned} \tag{7}$$

where the first term is the geometric delay corresponding to the reference direction $\boldsymbol{s_0}$, and the second term τ_s is the additional delay introduced by the extended brightness distribution. Thus, the absolute source position determined in VLBI astrometry is the position of the adopted reference direction $\boldsymbol{s_0}$ if delay structure corrections are modeled in this way. In practice, the delay structure corrections τ_s are determined as the slope of a straight line fitted to the individual structure phases calculated for each frequency channel used during the observations, in order to match precisely the scheme used to build the bandwidth synthesis delay observable at the correlator (see [5]). The effect introduced by the extended source brightness distribution in the phase-delay rate, defined by the partial derivative of the total phase with respect to time, is obtained in a similar way, and must also be accounted for in a complete astrometric analysis. The interested reader is referred to [5] for a more thorough discussion of the phase-delay rate observable.

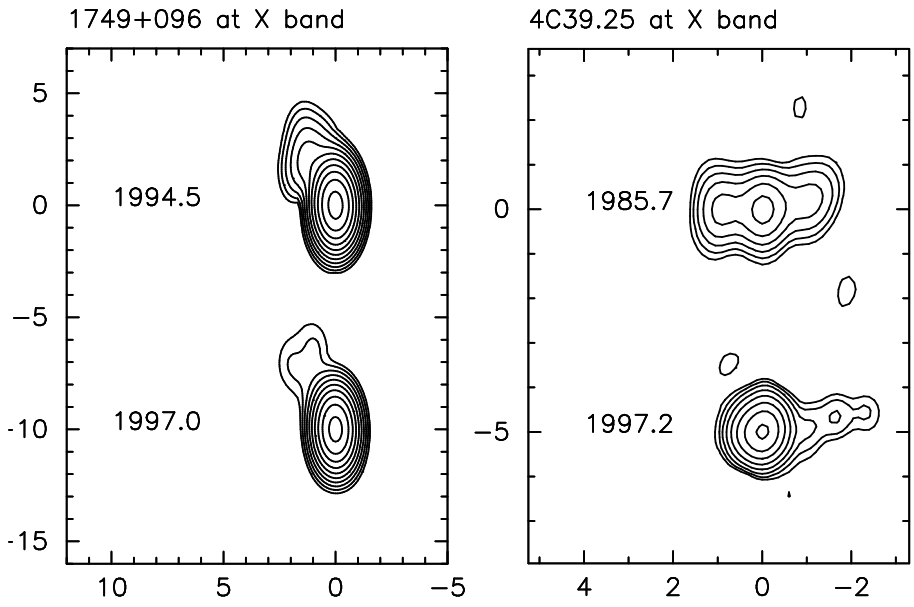

Figure 1. X-band VLBI maps at two epochs for the core-dominated source 1749+096 [1, 3] and the complex source 0923+392 (4C 39.25) [7]. The two maps in each panel are aligned vertically according to their peak brightness. The scale is in milliarcseconds.

In the case of dual-frequency S/X observations, the combined S/X structure correction is derived by combining the individual X- and S-band structure corrections with the same scale factors as those used to derive the dual-frequency-calibrated delay from the X- and S-band delay measurements. These factors are approximately 1.08 for the X-band delay and 0.08 for the S-band delay. The S-band structure corrections are therefore scaled by a factor of $0.08/1.08 \sim 1/13$ relatively to the X-band corrections, which limits their overall impact in the combined S/X corrections. Such a combination implies indeed that the same reference direction is selected for the X and S bands.

3. Choice of the Reference Direction

Calculation of source structure corrections requires the choice of a reference direction $\boldsymbol{s_0}$ within the source brightness distribution. As discussed previously, this reference direction is equivalent to the absolute position of the source in the extragalactic reference frame. An appropriate choice of the reference direction is critical for the source position stability since the absolute positions of the source brightness distributions are unknown with respect to the celestial frame. For sources with time-variable structure, it is important that this reference direction be set to a truly kinematically-stable morphological feature well identified over time. The identification of such a feature, however, is sometimes hard, for example in the case of core-jet sources with blended core and jet components, or for sources which change morphology over time.

Figure 1 illustrates the question of the reference direction for two different sources, 1749+096 and 0923+392 (4C 39.25). In the case of 1749+096, the peak brightness is a reasonable choice for the reference direction, as the brightness distribution is core-dominated and has evolved little between the two epochs. On the other hand, 0923+392 shows a totally different morphology at the

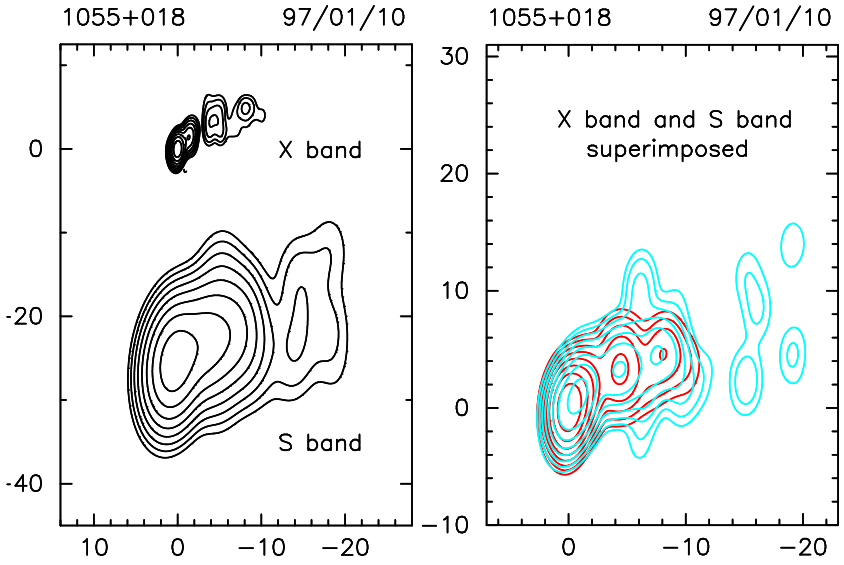

Figure 2. X- and S-band VLBI maps of the source 1055+018 [3]. The scale is in milliarcseconds. *Left:* Images convolved with a different beam at each frequency, reflecting the corresponding interferometer resolution. *Right:* Tentative superimposition of the two maps after convolution with the same beam (the S-band map, in blue/light grey was superresolved by a factor of 1.9, whereas the X-band map, in red/dark grey was underresolved by the same factor).

first epoch (triple structure) and at the second epoch (single component with a weak extension), making the cross-identification of the components largely impossible without information about the structure evolution at intermediate epochs. For this source, it turns out that the strongest component seen at the second epoch corresponds to the eastern (left-hand side) component of the earlier map [6, 7]. Registration of the two maps based on the peak brightness, as proposed in Fig. 1, is therefore not correct and would lead to inconsistent coordinates between the two epochs.

The calculation of dual-frequency S/X structure corrections similarly requires correct registration of the X- and S-band maps. This may even be harder than time registration, due to the difference in resolution, and because source structure is often significantly different at the two frequencies. Figure 2 illustrates such difficulty for the source 1055+018. On the left-hand side, the X- and S-band maps are plotted at the same scale, each convolved with a beam reflecting the intrinsic frequency-dependent interferometer resolution, while on the right-hand side, they are superimposed after convolution with an identical beam. It is evident from this figure that the peaks of the three detected components cannot be superimposed at once, as a consequence, most probably, of opacity variations within the structure. This makes registration errors inescapable, but fortunately these are attenuated in actual data analysis, as they are reduced by a factor of 13, like the S-band structure corrections, when deriving the combined S/X structure corrections (see Section 2).

The examples discussed above show that modeling radio source structure has two basic requirements: *(i)* regular VLBI monitoring to track source structure evolution, and *(ii)* a careful examination of each map to identify the proper reference direction for each source. The influence of the choice of the reference direction on actual VLBI results will be discussed further in Section 5.

4. Magnitude of Source Structure Effects

The theoretical modeling developed in Section 2 shows that source structure corrections depend on the exact form of the spatial brightness distribution of the extended radio source $I(\boldsymbol{s}, \omega, t)$ relative to the geometry of the VLBI baseline vector $\boldsymbol{b}$ projected onto the plane of the sky (see Equations (5) and (7)). The overall source structure effect magnitude for a given source is then most easily estimated by calculating these corrections for a range of u, v coordinates (the coordinates u and v are the coordinates of the baseline vector $\boldsymbol{b}$ projected onto the plane of the sky and are expressed in units of the observing wavelength). Along this direction, we defined a source "structure index" according to the median value of the structure delay corrections, $\tau_{\rm median}$, calculated for all projected VLBI baselines that could be possibly observed with Earth-based VLBI (i.e. for all baselines with $\sqrt{u^2+v^2}$ less than the diameter of the Earth), separating the sources into four classes as follows:

$$\text{Structure Index} \;=\; \begin{cases} 1, & \text{if } 0 \text{ ps} \le \tau_{\rm median} < 3 \text{ ps}, \\ 2, & \text{if } 3 \text{ ps} \le \tau_{\rm median} < 10 \text{ ps}, \\ 3, & \text{if } 10 \text{ ps} \le \tau_{\rm median} < 30 \text{ ps}, \\ 4, & \text{if } 30 \text{ ps} \le \tau_{\rm median} < \infty. \end{cases} \qquad [2]$$

Based on this definition, two structure indices are obtained for each source, one at X-band and one at S-band, each of which provides an indication of the source structure effect magnitude at the corresponding frequency band. For consistency with the procedure used to derive the dual-frequency structure corrections (see above), the structure corrections are scaled by 1.08 at X-band and by 0.08 at S-band, prior to the structure index assignment.

Shown in Fig. 3 are contour plots of the radio emission at X-band of four sources (0138−097, 0108+388, 0544+273 and 2201+315) representative of each structure index class. The corresponding structure-effect maps showing the magnitude of the corrections to the VLBI delay observable as a function of the interferometer resolution are also represented along with indication of the mean, rms, median and maximum values of these structure corrections. Figure 3 reflects the increase of the magnitude of the structure effects as the brightness distribution becomes more extended. For 0108+388, these effects are very large because the source structure is composed of two components of approximately equal strength, causing very low visibility regions in the u-v plane and thus large structure corrections (see [5] for a detailed study of the case of a two-component model).

Figure 4 shows the overall structure index distribution at X- and S- bands for the 392 sources of the International Celestial Reference Frame (ICRF) [4] that have currently available structure indices. At X-band, it is shown that approximately 60% of the sources in this sample have a structure index of either 1 or 2, an indication of compact or very compact structures, while the remaining 40% of the sources with a structure index of either 3 or 4 have more extended emission structures. At S-band, source structure effects appear to be less significant, as reflected by the large number of sources with a S-band structure index of either 1 or 2 in Fig. 4 (about 90% of the sources). This is an indirect indication that the contribution of the S-band structure to the dual-frequency-calibrated delay is usually smaller as compared to the X-band structure contribution, a consequence of the fact that the S-band structure corrections have been scaled by a factor of 0.08.

In all, it is recommended that only sources with a structure index of either 1 or 2 be used for the most precise astrometric or geodetic work [2, 3]. Sources with a structure index of 3 should only be used with caution while those with a structure index of 4 should not be used at all.

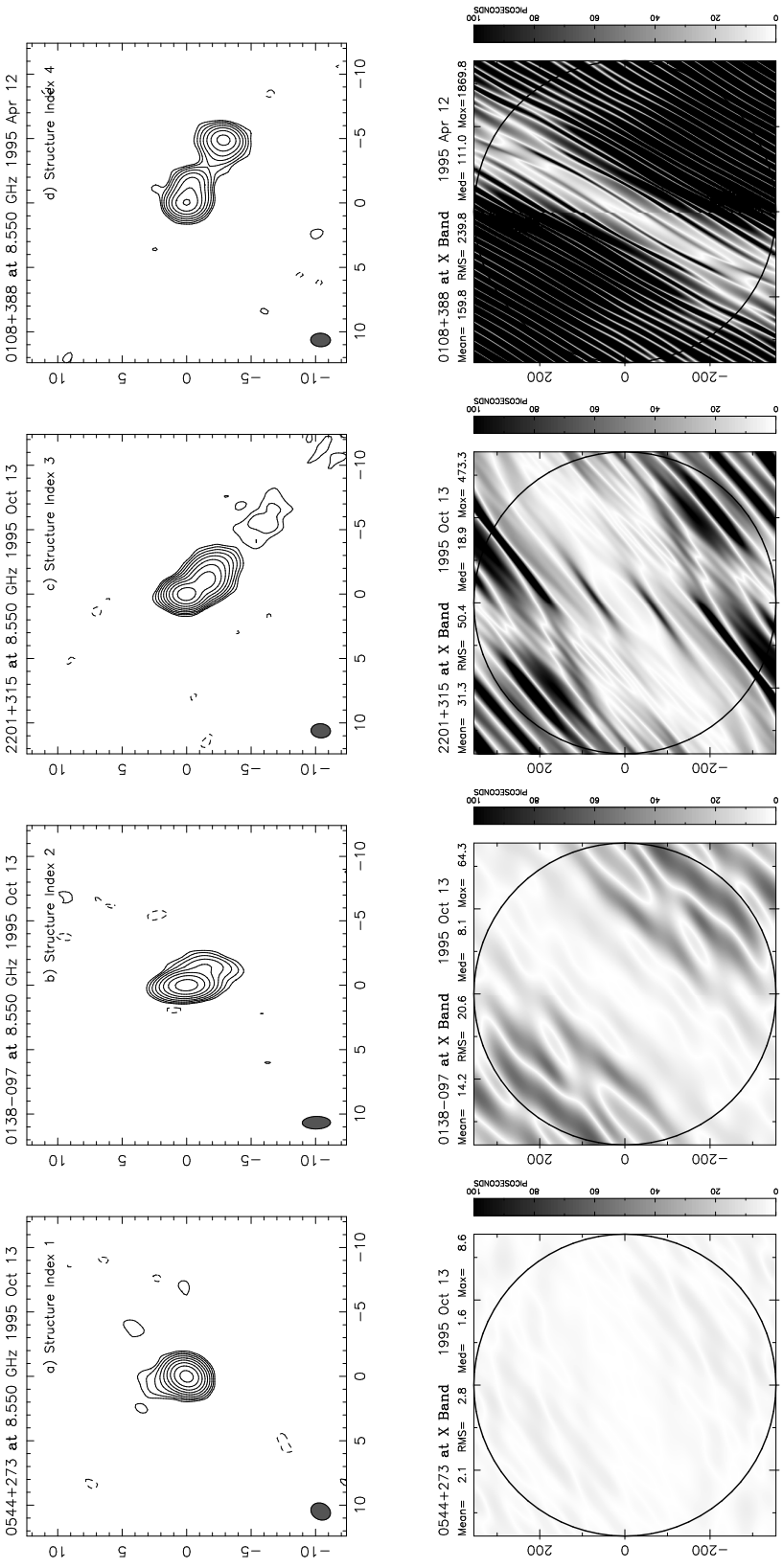

Figure 3. *Top:* Contour plots of the radio emission at X-band for the four sources a) 0544+273, b) 0138−097, c) 2201+315 and d) 0108+388, representative of each structure index class. The X-band structure index of these sources in indicated in each panel. *Bottom:* Gray-scale plots showing the magnitude of the structural delays (absolute value) induced by the extended radio emission at X-band for the same four sources. The structural delay is plotted as a function of the length and orientation of the VLBI baseline projected onto the sky, expressed in millions of wavelengths (u, v coordinates). The gray scale is identical in each panel and ranges from 0 to 100 picoseconds (ps). All structure corrections larger than 100 ps are plotted as black. The circle drawn in these plots has a radius equal to one Earth diameter, corresponding to the longest baselines that can be theoretically observed with Earth-based VLBI. The mean, rms, median and maximum values of the structure corrections for all baselines contained within this circle are indicated in each panel.

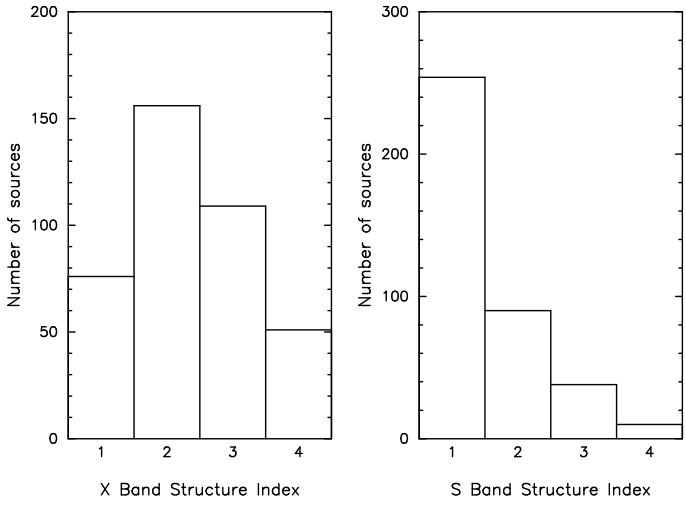

Figure 4. Distribution of the X- and S-band structure indices for 392 ICRF sources.

5. Modeling Structure Delays in Actual VLBI Observations

While the structure index is useful for planning experiments and estimating the extra noise caused by source structure in existing data, the ultimate goal is indeed to directly apply structure corrections to actual observations. A first step in this direction was made by using data from the mid-80s on the extended core-jet source 3C273 (1223+026), intensively observed in geodetic experiments at that time. The results of this initial study, based on two years of data, showed that modeling structure effects significantly improves the positional stability of 3C273 and reduces the rms delay residuals [8]. More recently, a similar analysis was carried out for the source 4C39.25 (0923+392) using a longer data span (12 years of observations) [7]. This source has been known for its peculiar systematic long term proper motion in right ascension with an average value of ~ 0.06 mas/yr [9]. After incorporating source structure modeling, this proper motion was found to largely vanish, confirming that it is not real, but caused by source structure evolution [7].

Just recently, such exploratory studies have been extended to a much larger scale with a data set consisting of the first 10 RDV sessions, including 160 sources observed over up to all 10 epochs and a total of $\sim 200,000$ observations [10]. This massive analysis made use of 800 maps from the Radio Reference Frame Image Data Base of the US Naval Observatory [11] produced from the same 10 RDV experiments. Overall, the weighted rms delay residuals (~ 30 ps) were found to decrease by 8 ps in quadrature upon introducing source maps to model the structure delays, with improvements as large as 40 ps for some sources with extended or fast-varying structures. Scatter of "arc positions" about a time-linear model were also found to decrease substantially for most sources. While a complete description of this analysis and overall statistical results are given in [10], we report here further details of our results for the source 2200+420.

The source 2200+420 was selected for this study because its data were found to be significantly affected by structural effects, thus providing a good case to test our software and illustrate specific questions like the impact of the choice of the reference direction on the results. Figure 5 shows the 10 successive X- and S-band VLBI maps of 2200+420 used in our analysis. At X-band, the source consists of two major components, whose relative position and strength apparently change

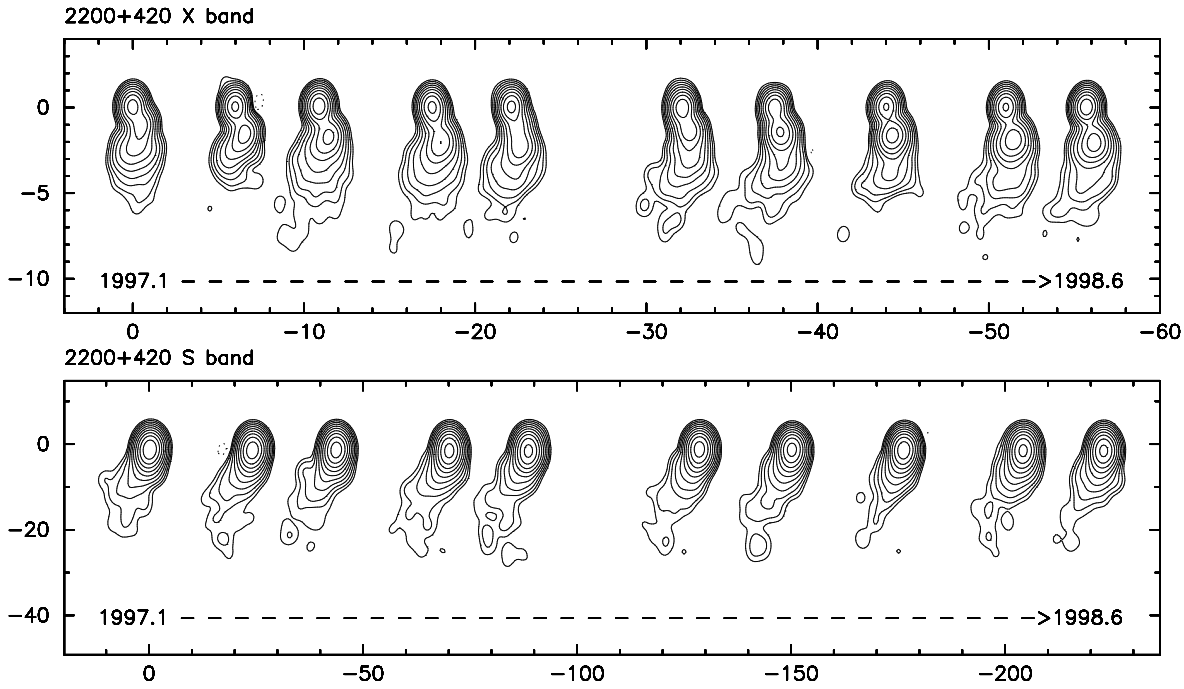

Figure 5. VLBI images of 2200+420 at X band (top) and S band (bottom) for 10 successive epochs, spanning the period 1997.1–1998.6, as available from [11]. The maps are aligned horizontally according to the northern structural component and are spaced linearly according to their observing epochs. The scale is in milliarcseconds.

over time. The northern component is generally stronger, except for the maps at epochs 7 and 8. At S-band, the source structure is similar, but the two major components are blended due to the weaker resolution at this frequency.

We have conducted four successive astrometric analyses estimating "arc positions" of 2200+420, one of which (solution **a**) did not incorporate structural delay modeling, while the three others (solutions **b**, **c** and **d**) had structural delays modeled via the source maps in Fig. 5. The difference between solutions **b**, **c** and **d** lies in the choice of the reference direction, which was either set on the peak brightness (solution **b**) or the brightness centroid (solution **c**) using an automatic procedure, or chosen *manually* after a careful examination of each map aimed at locating the most-likely stable fiducial feature within the source extended structure (solution **d**). This led us to select the northern map component (at both X- and S-bands) for the latter, under the assumption that this feature constitutes the source core.

The results of these four "arc positions" astrometric analyses are plotted in Fig. 6. Without structural delay modeling (solution **a**), the rms position scatter is 0.0080 ms for right ascension and 0.41 mas for declination. The larger scatter in declination is due mostly to the estimated positions at epochs 7 and 8, which are off by 0.5 to 1 mas from the other estimated positions. When modeling structure delays, source position scatter is either substantially worse (solution **b**) or largely improved with quasi-perfect correction of the shifts for epochs 7 and 8 (solutions **c** and **d**), indicating that these are really an effect of extended structure. Degraded scatter in solution **b** obviously originates in inconsistent choice of the reference direction, fixed to the southern

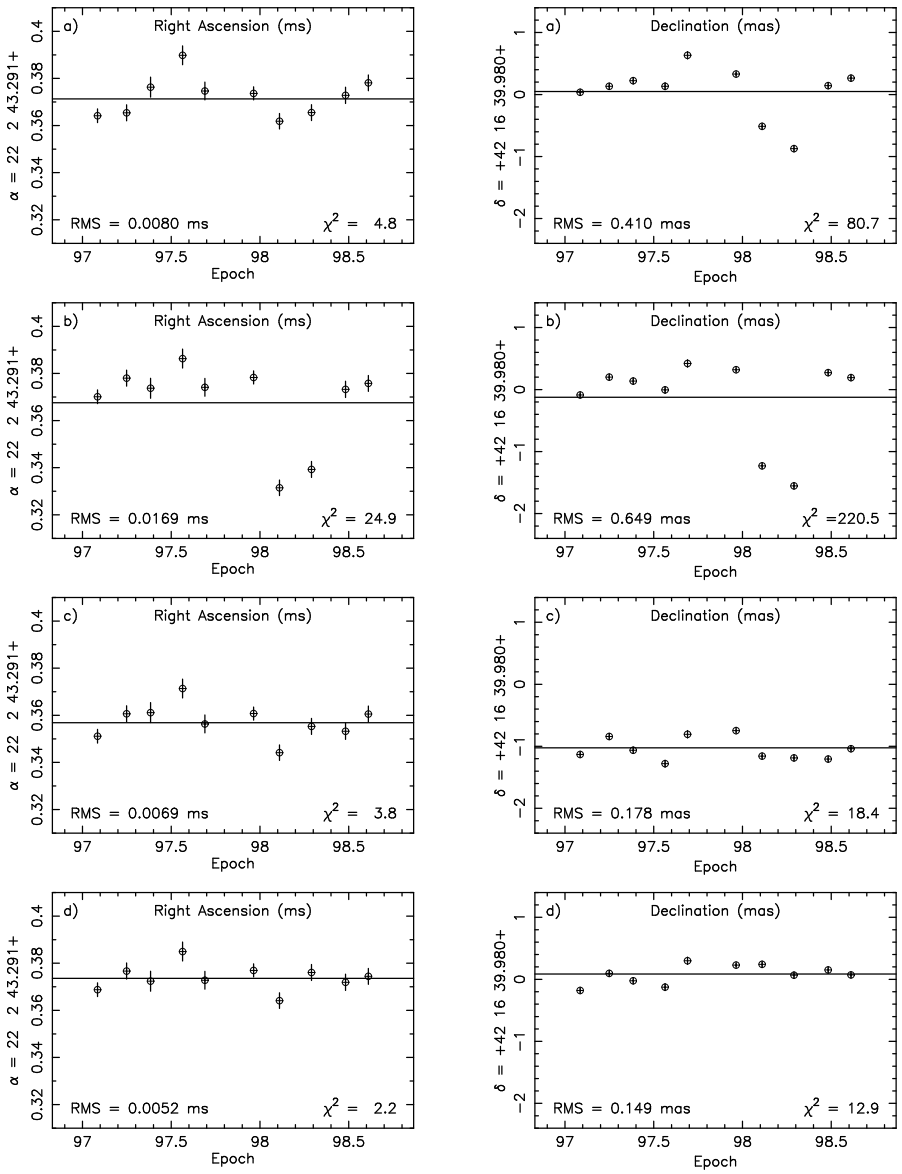

Figure 6. Estimated right ascension and declination of 2200+420 for 10 successive epochs, spanning the period 1997.1–1998.6. Source structure is modeled using the VLBI maps from Fig. 5 with the following specifications: a) no modeling, b) map peak as reference direction, c) brightness centroid as reference direction, d) northern structure component as reference direction.

structure component at epochs 7 and 8 and to the northern component at all other epochs, as a result of the peak brightness "blind" selection. Overall, the smallest position scatter is obtained for solution **d** when selecting the northern structural component as the source reference direction. In this case, scatter is reduced from 0.0080 to 0.0052 ms in right ascension and from 0.41 to 0.15 mas in declination (along with large decrease in χ^2 per degree of freedom values) upon modeling structural delays (Fig. 6), thus indicating that such modeling really improves the source position stability.

6. Conclusion

The analyses carried out so far to evaluate the magnitude of the source structure effects, based on the modeling described in Section 2, indicate that these effects are significant. Structural delays range from a few picoseconds for the most compact sources to several hundreds of picoseconds for the very extended sources. In this connection, the structure index defined in [2, 3] is a useful indicator to evaluate the source quality. About 60% of the ICRF sources evaluated in this way are found to have structure indices of either 1 or 2, making them suitable for high-precision astrometry.

Additionally, it has now been demonstrated that massive application of structure maps to correct for structural delays is possible and improves VLBI analysis, predominantely for sources with extended structures [10]. The specific case of 2200+420 discussed in Section 5 shows that identification of a true fiducial feature within each extended source is crucial to properly and accurately model structural delays, as otherwise the results may be worse than with no structure corrections. Future plans should especially focus on such identification so that analyses incorporating massive source structure modeling like that described in [10] can be further improved.

References

[1] Fey, A. L., Clegg, A. W., Fomalont, E. B., 1996, VLBA Observations of Radio Reference Frame Sources, ApJS, 105, 299–330.

[2] Fey, A. L., Charlot, P., 1997, VLBA Observations of Radio Reference Frame Sources. II. Astrometric Suitability Based on Observed Structure, ApJS, 111, 95–142.

[3] Fey, A. L., Charlot, P., 2000, VLBA Observations of Radio Reference Frame Sources. III. Astrometric Suitability of an Additional 225 Sources, ApJS, 128, 17–83.

[4] Ma, C., Arias, E. F., Eubanks, T. M., Fey, A. L., Gontier, A.-M., Jacobs, C. S., Sovers, O. J., Archinal, B. A., Charlot, P., 1998, The International Celestial Reference Frame as Realized by Very Long Baseline Interferometry, AJ, 116, 516–546.

[5] Charlot, P., 1990, Radio-Source Structure in Astrometric and Geodetic Very Long Baseline Interferometry, AJ, 99, 1309–1326.

[6] Guirado, J. C., Marcaide, J. M., Alberdi, A., Elósegui, P., Ratner, M. I., Shapiro, I. I., Kilger, R., Mantovani, F., Venturi, T., Rius, A., Ros, E., Trigilio, C., Whitney, A. R., 1995, Proper Motion of Components in 4C 39.25, AJ, 110, 2586–2596.

[7] Charlot, P., 2000, Models for Source Structure Corrections, in Proceedings of IAU Colloquium 180, Towards Models and Constants for Sub-microarcsecond Astrometry, Eds. K. J. Johnston, D. D. McCarthy, B. J. Luzum and G. H. Kaplan, U. S. Naval Observatory, Washington, D. C., p. 29–39.

[8] Charlot, P., 1994, Evidence for Source Structure Effects Caused by the Quasar 3C273 in Geodetic VLBI Data, in VLBI Technology – Progress and Future Observational Possibilities, Eds. T. Sasao, S. Manabe, O. Kameya, and M. Inoue, Tokyo: Terra Scientific Publishing Company, p. 287–294.

[9] Fey, A. L., Eubanks, T. M., Kingham, K. A., 1997, The Proper Motion of 4C 39.25, AJ, 114, 2284–2291.

[10] Sovers, O. J., Charlot, P., Fey, A. L., Gordon, D., 2002, Structure Corrections in Modeling VLBI Delays for RDV data, these proceedings.

[11] Fey, A. L., Boboltz, D., Gaume, R., Kingham, K. A., 2002, USNO Analysis Center for Source Structure Report, International VLBI Service for Geodesy and Astrometry 2001 Annual Report, Eds. N. R. Vandenberg and K. D. Baver, NASA/TP-2002-210001 (in press).